

Screening of druggable conformers of α -synuclein using molecular dynamics simulationDorothy Das¹ , Mridusmita Kakati¹ , Aroon Gracy² , Airy Sanjeev¹ , Swarna Mayee Patra³ , Venkata Satish Kumar Mattaparthi¹ ¹Molecular Modelling and Simulation Laboratory, Department of Molecular Biology and Biotechnology, Tezpur University, Tezpur-784 028, Assam, India²Department of Biotechnology, Bharathidasan University, Tiruchirapalli- 620 024, Tamil Nadu, India³Department of Chemistry, R V Engineering College, Mysuru Road, Bengaluru, Karnataka 560 059, India*corresponding author e-mail address: mvenkatasatishkumar@gmail.com, venkata@tezu.ernet.in | Scopus ID: [54962670000](https://orcid.org/0000-0002-5496-2670)

ABSTRACT

Intrinsically disordered proteins (IDPs) are becoming an engaging prospect for therapeutic intervention by small drug-like molecules. IDPs structural binding pockets and their flexibility exist as a challenging target for standard druggable approaches. Hence, in this study, we have performed and identified the most probable druggable conformers from molecular dynamics simulation on α -synuclein based on the structural parameters: radius of gyration (R_g), solvent accessible surface area (SASA) and the standard secondary structure content. We found the conformers showing lower solvent accessible surface area and higher secondary structure content of α -helical are defined to be suitable binding pockets for druggability.

Keywords: α -synuclein; druggability; intrinsically disordered proteins; molecular dynamics.

1. INTRODUCTION

Intrinsically disordered proteins (IDPs) exhibit prevalent key roles in the biological processes of all diversified living organisms. IDPs are broadly involved in crucial cellular activities, including regulation and signal transduction [1] and are also linked with a number of human diseases [2-4] such as in expression of cancer related proteins (p53, breast cancer protein BRCA-1/2) and other neurodegenerative disorders including the α -synuclein and tau protein in Alzheimer's disease [5]. IDPs structural attributes of high flexibility and lack of stable secondary and tertiary structures, often engaged themselves at the hubs of protein-protein interaction networks and consequently associates with multiple partners [6-8]. The primary step of fibrillogenesis of IDPs requires the stabilization of monomeric or oligomeric partially folded conformations as they are devoid of a stable structure. As Statistically stated, 79% of malignancy related proteins and 57% of the distinguished cardiovascular disease-related proteins are anticipated to contain shorter regions which are disordered and no longer than 30 residues in length [9-10]. Therefore, IDPs can be perceived as active drug targets and to play a significant role in drug design [11-25]. However, prior to drug design on a specific protein it is crucial to evaluate its possibility to be a decent drug target. Also, presence of binding cavities of appropriate geometrical shape for ligand binding ("druggability"), acts as a crucial assessment problem in drug discovery [26]. Therefore the drug design strategy for IDPs are yet in their early stages [27] in comparison with the ordered proteins for which there exists well-developed drug design pipelines[28]. In IDPs, the number of binding cavities were predicted to be more in number than in the case of ordered proteins of similar length. In addition, from the literature review studies, it is evident that the cavities of IDPs exerting greater surface areas and larger volumes shows higher druggability than those of ordered proteins. In addition, IDPs must possess important biological roles and establish their association with the specific disorder, which aids in drug designing towards

IDPs. The obstacles along with the possible measures in designing the drugs for IDPs have been reported [5]. Although there are few limitations developed during drug designing targeted IDPs of which major defaults were lack of efficient experimental screening strategies and determining specificity that impacts ligand-protein interactions. The enzymes and cell surface receptors become the target of the most of the drugs by regulating their functions, wherein the small molecules can mimic the interactions made by their natural substrates [29]. Even though enzymes possess a certain degree of flexibility, their structures tend to fluctuate around equilibrium positions, making it easier to identify binding pockets and subsequently design drugs to fit in them. On the other hand, IDPs exist as large ensembles of structures, where their amino acid chains can rapidly form multiple conformations, sometimes within microseconds. They exhibit large conformational fluctuations and no evidence of permanent binding pockets. This type of conformational feature does not present suitable cavities for small drug-like molecules to form stable interactions [13-14, 30-31]. IDPs are frequently striking different postures. Allowing their highly dynamic nature into consideration, we have performed Molecular dynamics simulation on α -synuclein protein, a typical IDP, to get a better sampling of conformers. The compactness of a protein which is measured as Radius of gyration (R_g) is known to affect the stability and folding rate of proteins [32]. In addition to this, recent studies have reported the use of compactness to define the binding pockets in a protein [33-35]. Some of the studies have highlighted the idea of considering compactness (R_g) of the protein or protein-ligand complexes for binding site prediction [33,35]. Recent studies suggest that lower the R_g , the compactness of the ligand-protein complex is higher, causing the interactions between ligand and protein to be stronger [34]. Also, R_g depicts the significance of a more compact well-docked protein-ligand complex to be a better therapeutic agent [36]. Structure-based prediction of ligand

binding sites approaches has also been reported to focus on designing consensus that includes the shape of the input protein fold, expressed by its R_g , as one of its features [37]. In our study, we have performed 80 ns of molecular dynamic simulation on α -synuclein protein to analyze the conformational properties. From

2. MATERIALS AND METHODS

2.1. MD Simulation.

The MD study was carried out using a standard procedure, where the energy minimized structure of α -synuclein was subjected to heating, equilibration and production dynamics. The system was gradually heated from 0-300 K in constant volume (NVT) conditions and then equilibration was conducted in NPT conditions (300 K and 1 atm pressure). To ensure the correctness of our NPT simulation protocol, the density, temperature, pressure, energy and RMSD (Root Mean Square Deviation) graphs were plotted and analyzed (shown in **Figure S1-S5**). Then 80 ns MD production run was carried out on the equilibrated structure using the Particle Mesh Ewald (PME) algorithm [38,39] with the time step of 2 fs. To treat the nonbonding interactions (short-range electrostatic and van der Waals interactions) a cutoff of 8 Å was used during the simulation while the long-range electrostatic interactions were treated with the PME method. All the bonds present in the system were constrained with the SHAKE algorithm [40]. The pressure and temperature (0.5 ps of heat bath and 0.2 ps of pressure relaxation) were held constant by the Berendsen weak coupling algorithm [41] throughout the simulation process. The trajectory analysis of the system was carried out using cpptraj program [42] from AmberTools.

2.2. Clustering of Conformers based on R_g .

In order to identify the druggable conformer of α -synuclein protein from MD simulation trajectory, we have screened the

3. RESULTS

In this study, we have screened the conformers of α -synuclein protein from the MD simulation trajectory that exhibit well defined binding pockets necessary for druggability.

3.1. Radius of gyration Analysis.

To investigate the compactness of α -synuclein protein during the simulation, radius of gyration was analyzed. Information regarding the overall shape and size of the molecule can be gleaned from R_g . The radius of gyration analysis for α -synuclein protein as a function of simulation time is shown in **Figure 1**.

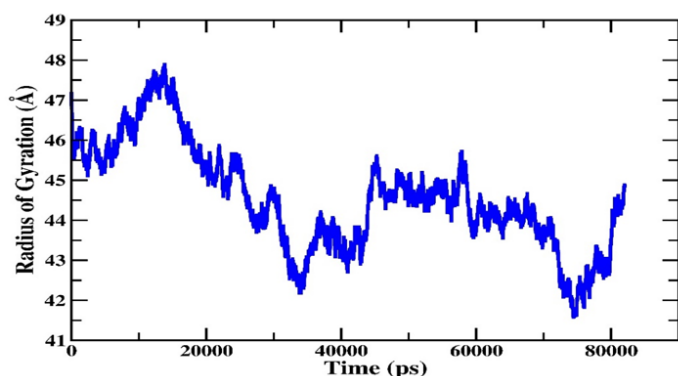


Figure 1. Radius of Gyration analysis for α -synuclein as a function of simulation time.

the MD simulation trajectory, the probable conformers of α -synuclein having druggable features have been isolated based on the structural parameters; R_g , solvent accessible surface area (SASA) and moderate standard secondary structure content.

conformers based on R_g values and grouped them into three clusters: L group (conformers having lower R_g values), M group (conformers having moderate R_g values) and H group (conformers having higher R_g values). For this study, we have pulled out the bottom five conformers depicted as L1-L5 from L group. Similarly, from M group and H group we have pulled out the top five conformers depicted as M1-M5 and H1-H5, respectively. To obtain information regarding the buried and exposed area present in each of these conformers, solvent accessible surface area (SASA) analysis was carried out using cpptraj program.

2.3. Prediction of Binding pockets.

The conformers in the clusters were analyzed using the online server tool CASTp (Computed Atlas of Surface Topography of proteins) [43] that detects, measures and provides a detailed characterization of the binding pockets on the surface of the proteins as well as the voids in the interior of proteins. Usually, these surface pockets and voids that correlate with binding activities are the concave regions of the proteins. CASTp server determines all the surface pockets and voids present in the structure of proteins using an algorithm that focus on alpha shape and pocket. This algorithm was developed in computational geometry. This server describes the surface pockets as concave regions of proteins with binding sites at the opening. These pockets also allow access to water molecules from the exterior.

The R_g value is known to affect both the stability and folding rate of a protein. From **Figure 1**, we can infer that the R_g value of α -synuclein to oscillate within the range of 41 Å to 48 Å during the course of simulation. In order to isolate the probable conformers of α -synuclein featuring druggability, the conformers from the MD simulation trajectory were clustered according to their R_g values. Conformers L1-L5, M1-M5 and H1-H5 were selected from the clusters of lower, moderate and higher values of R_g , respectively.

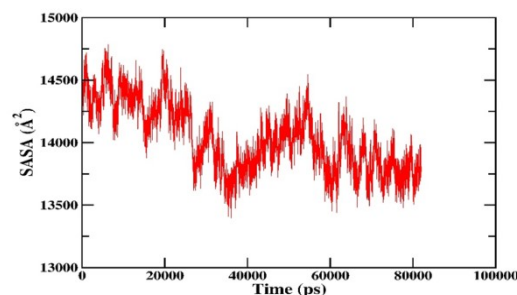


Figure 2. SASA analysis for α -synuclein as function of simulation time.

3.2. Solvent accessible surface area Analysis.

In order to investigate the absolute details about the mobility of flexible regions in α -synuclein protein, we calculated SASA from MD simulation trajectory using cpptraj program. The results were depicted in **Figure 2**. From **Figure 2**, we can infer

that the SASA value of α -synuclein takes the value in the range of 13400 \AA^2 to 14800 \AA^2 . Hence, it depicted that the mobility of flexible regions in α -synuclein protein was observed in the range of 13400 \AA^2 to 14800 \AA^2 . It can be correlated with Table 1 with the number of R_g and binding pockets.

3.3. Binding Pocket Analysis.

Binding pockets in the screened conformers of α -synuclein having lower (L1-L5), moderate R_g (M1-M5) and higher R_g (H1-H5) values have been predicted with the help of CASTp server and results were depicted in **Figure 3**. In **Table 1**, we have summarized the R_g , SASA and the number of binding pockets of the corresponding screened conformers of α -synuclein. From **Table 1**, we observe the number of binding pockets to be more in the conformers having lower R_g values than conformers having higher R_g values. Also, we notice the conformers having lesser SASA values to contain more binding pockets. Hence, we observe that among H, M and L group, the conformers under Group L contain a greater number of well-defined binding pockets. From these observations, we can infer that R_g and SASA value of the protein may be considered as critical aspects for identifying the conformers having druggable features.

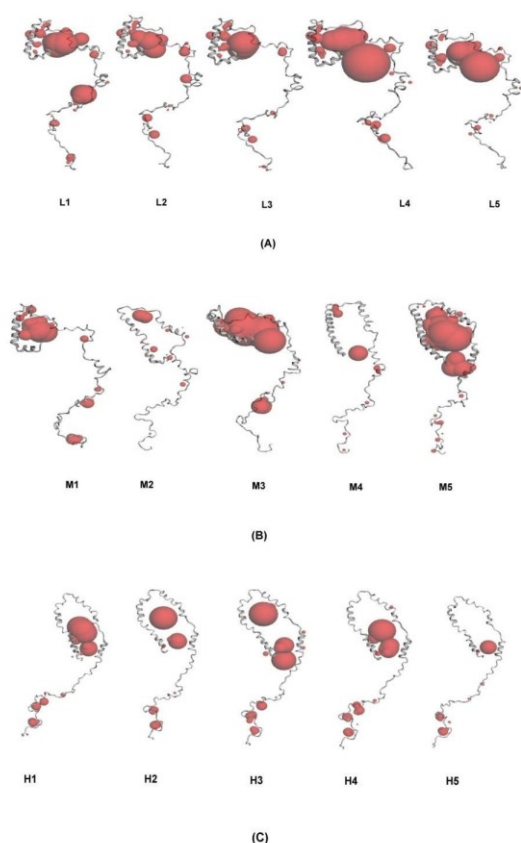


Figure 3. Binding pocket analysis for the conformers of α -synuclein having (A) Lower R_g values (B) Moderate R_g values. (C) Higher R_g values.

3.4. Secondary Structure Analysis.

The Secondary structure analysis was carried out using the Kabsch and Sander algorithm [44] incorporated in their DSSP (Dictionary of secondary structure for proteins) program. The results were plotted in **Figure 4**. The plot shows the structural variation of each residue during the time course of the simulation. From **Figure 4**, we observe that α -helix secondary structure was mostly retained in the N-terminal region of the protein while in the

NAC and C-terminal region there were rapid transitions from one secondary structure to another.

Table 1. R_g , SASA and Number of binding pockets for the screened conformers of α -synuclein having lower, middle and higher R_g values

CONFORMERS	R_g VALUES (\AA)	SASA VALUES (\AA^2)	NUMBER OF BINDING POCKETS
L1	41.582	13692.33	15
L2	41.588	13748.63	17
L3	41.597	13728.49	11
L4	41.599	13791.03	19
L5	41.603	13798.73	16
M1	42.997	13973.61	9
M2	43.999	13804.06	10
M3	44.998	13862.44	11
M4	45.973	14255.19	7
M5	46.041	14655.89	15
H1	47.895	14494.96	11
H2	47.868	14477.31	7
H3	47.868	14341.28	11
H4	47.864	14377.58	9
H5	47.855	14415.70	8

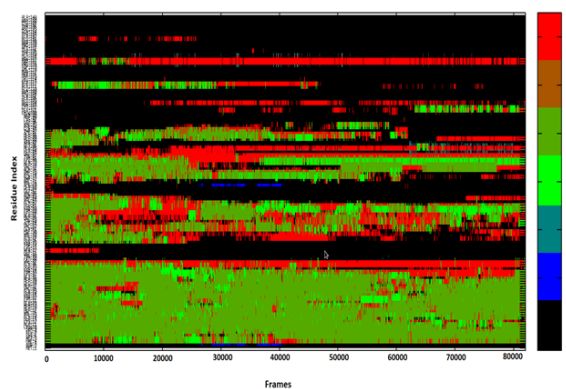


Figure 4. The evolution of secondary structure evaluated using DSSP is shown for α -synuclein. Y-axis depicts residues and X-axis depicts time frames during the course of MD simulation. The secondary structure components of α -synuclein are color-coded as shown in the panel.

We have also calculated the percentage of individual secondary structure content across the screened conformers using YASARA software [45]. Considering both the secondary structure content and number of binding pockets in the screened conformers, we have summarized the results in **Table 2**. From **Table 2**, it can be observed that L4 in spite of having a comparatively higher R_g value than the other conformers in that group, was estimated to contain relatively a greater number of binding pockets. This is the same for M5 and H3 under the group M and H respectively. We found that in all these conformers (L4, M5 and H3), the percentage of α -helical secondary structure content is relatively more than the other conformers in the corresponding groups. From these observations, we notice that the percentage of the standard secondary structure content, especially, α helical portion of the protein to play a significant role in influencing the occurrence of a number of binding pockets. The additional information about the geometry (area and volume), number of residues and atoms involved in the binding pockets of all the screened conformers have been summarized in **Table S1**. The binding cavities of IDPs were reported to have larger surface area and volume than the cavities of ordered proteins [5]. Therefore, conformers with lower R_g value, lesser solvent

accessible surface area and higher standard secondary structure content are more preferable to possess druggable features.

Table 2. Secondary structure content and the Number of Binding Pockets for the conformers of α -synuclein having lower, middle and higher R_g values.

CONFORMERS	SECONDARY STRUCTURES				NUMBER OF BINDING POCKETS
	HELIX (%)	SHEETS (%)	TURNS (%)	COILS (%)	
L1	21.4	0.0	14.3	64.3	15
L2	22.1	0.0	14.3	60.0	17
L3	17.9	0.0	22.9	59.3	11
L4	22.9	0.0	14.3	62.9	19
L5	17.9	0.0	14.3	65.0	16
M1	19.3	0.0	20.0	60.7	9
M2	20.7	0.0	22.9	52.9	10
M3	20.7	0.0	20.0	59.3	11
M4	26.4	0.0	11.4	59.3	7
M5	40.0	0.0	11.4	48.6	15
H1	12.9	0.0	31.4	55.7	11
H2	11.4	0.0	40.0	48.6	7
H3	21.4	0.0	25.7	52.9	11
H4	15.7	0.0	34.3	50.0	9
H5	12.1	0.0	25.7	59.3	8

4. CONCLUSIONS

In conclusion, we have demonstrated here that isolation of the most probable conformer of α -synuclein from structural molecular dynamic analysis/ based on some critical aspects that emphasizes on its nature of druggability as a potential drug target. Our observations have supported that conformers having lower values of R_g have a definitely greater number of binding pockets. With higher compactness of the structure, greater cavities are observed which are aided by the conformers. However, this is not the only factor that is solely responsible for the druggable nature of the protein molecule. Compactness coupled with the solvent accessible surface areas of the conformers and also their secondary structure content, are equally crucial attributes. Also,

the parameters of the binding pockets in a protein molecule, serve as an essential element to be considered for drug design approaches. In this study we have identified conformers of α -synuclein containing druggable features that can serve as an input in designing drug like molecules. Our findings interpreted an idealistic insight on defining the druggability of α -synuclein that can be anticipated for which it will be considered as a preferable target in drug discovery initiatives in the future. From the above references studied and to the best of our knowledge, the proposed strategy may be used as a potential method to characterize druggability and can be generalized to overcome the obstacles for drug design of other IDPs as well.

5. REFERENCES

- Xie, H., Vucetic, S., Iakoucheva, L. M., Oldfield, C. J., Dunker, A. K., Uversky, V. N., & Obradovic, Z. Functional anthology of intrinsic disorder. 1. Biological processes and functions of proteins with long disordered regions. *Journal of proteome research* **2007**, *6*, 1882-1898, <https://doi.org/10.1021/pr060392u>.
- Babu, M.M.; van der Lee, R.; de Groot, N.S.; Gsponer, J. Intrinsically disordered proteins: regulation and disease. *Current opinion in structural biology* **2011**, *21*, 432-440, <https://doi.org/10.1016/j.sbi.2011.03.011>.
- Mendoza-Espinosa, P.; Garcia-Gonzalez, V.; Moreno, A.; Castillo, R.; Mas-Oliva, J. Disorder-to-order conformational transitions in protein structure and its relationship to disease. *Molecular and cellular biochemistry* **2009**, *330*, 105-120, <https://doi.org/10.1007/s11010-009-0105-6>.
- Midic, U.; Oldfield, C.J.; Dunker, A.K.; Obradovic, Z.; Uversky, V.N. Protein disorder in the human diseaseome: unfoldomics of human genetic diseases. *Bmc Genomics* **2009**, *10*, S12, <https://doi.org/10.1186/1471-2164-10-s1-s12>.
- Zhang, Y.; Cao, H.; Liu, Z. Binding cavities and druggability of intrinsically disordered proteins. *Protein science* **2015**, *24*, 688-705, <https://doi.org/10.1002/pro.2641>
- Dunker, A.K.; Cortese, M.S.; Romero, P.; Iakoucheva, L.M.; Uversky, V.N. Flexible nets: the roles of intrinsic disorder in protein interaction networks. *The FEBS journal* **2005**, *272*, 5129-5148, <https://doi.org/10.1111/j.1742-4658.2005.04948.x>
- Malaney, P.; Pathak, R.R.; Xue, B.; Uversky, V.N.; Davé, V. Intrinsic disorder in PTEN and its interactome confers structural plasticity and functional versatility. *Scientific reports* **2013**, *3*, 2035, <https://doi.org/10.1038/srep02035>.
- Mészáros, B.; Simon, I.; Dosztányi, Z. The expanding view of protein-protein interactions: complexes involving intrinsically disordered proteins. *Physical biology* **2011**, *8*, <https://doi.org/10.1088/1478-3975/8/3/035003>
- Cheng, Y.; LeGall, T.; Oldfield, C.J.; Dunker, A.K.; Uversky, V.N. Abundance of intrinsic disorder in protein associated with cardiovascular disease. *Biochemistry* **2006**, *45*, 10448-10460, <https://doi.org/10.1021/bi060981d>
- Iakoucheva, L.M.; Brown, C.J.; Lawson, J.D.; Obradović, Z.; Dunker, A.K. Intrinsic disorder in cell-signaling and cancer-associated proteins. *Journal of molecular biology* **2002**, *323*, 573-584, [https://doi.org/10.1016/S0022-2836\(02\)00969-5](https://doi.org/10.1016/S0022-2836(02)00969-5).
- Cheng, Y.; LeGall, T.; Oldfield, C.J.; Mueller, J.P.; Van, Y.Y.J.; Romero, P.; Cortese, M.S.; Uversky, V.N.; Dunker, A.K. Rational drug design via intrinsically disordered protein. *Trends in biotechnology* **2006**, *24*, 435-442 <https://doi.org/10.1016/j.tibtech.2006.07.005>.

12. Chen, C.Y.C.; Tou, W.I. How to design a drug for the disordered proteins? *Drug Discovery Today* **2013**, *18*, 910-915, <https://doi.org/10.1016/j.drudis.2013.04.008>
13. Dunker, A.K.; Uversky, V.N. Drugs for 'protein clouds': targeting intrinsically disordered transcription factors. *Current opinion in pharmacology* **2010**, *10*, 782-788, <https://doi.org/10.1016/j.coph.2010.09.005>.
14. Metallo, S.J. Intrinsically disordered proteins are potential drug targets. *Current opinion in chemical biology* **2010**, *14*, 481-488, <https://doi.org/10.1016/j.cbpa.2010.06.169>
15. Uversky, V.N.; Oldfield, C.J.; Dunker, A.K. Intrinsically Disordered Proteins in Human Diseases: Introducing the D2 Concept. *Annual Review of Biophysics* **2008**, *37*, 215–24. <https://doi.org/10.1146/annurev.biophys.37.032807.125924>.
16. Wang, J.; Cao, Z.; Zhao, L.; Li, S. Novel strategies for drug discovery based on intrinsically disordered proteins (IDPs). *International journal of molecular sciences* **2011**, *12*, 3205-3219, <https://doi.org/10.3390/ijms12053205>.
17. Santofimia-Castano P, Xia Y, Lan W, Zhou Z, Huang C, Peng L, Soubeyran P, Velázquez-Campoy A, Abián O, Rizzuti B et al Ligand-based design identifies a potent NUPR1 inhibitor exerting anticancer activity via necroptosis. *J Clin Invest* **2019** 130:2500–2513 <https://doi.org/10.1172/JCI127223>
18. Santofimia-Castano P, Lan W, Bintz J, Gayet O, Carrier A, Lomberk G, Neira JL, González A, Urrutia R, Soubeyran P, Iovanna JL Inactivation of NUPR1 promotes cell death by coupling ER-stress responses with necrosis. *Scientific Reports* **2018** 8:16999 <https://doi.org/10.1038/s41598-018-35020-3>.
19. Ruan H, Sun Q, Zhang W, Liu Y, Lai L (2019) Targeting intrinsically disordered proteins at the edge of chaos. *Drug Discov Today* **2019** 24:217–227 <https://doi.org/10.1016/j.drudis.2018.09.017>.
20. Jordi Pulos, et al; Small molecule inhibits α -synuclein aggregation, disrupts amyloid fibrils, and prevents degeneration of dopaminergic neurons, *PNAS*, **2018** 115 (41)10481-10486 <https://doi.org/10.1073/pnas.1804198115>
21. Diana L Price et al The small molecule alpha-synuclein misfolding inhibitor, NPT200-11, produces multiple benefits in an animal model of Parkinson's disease *Scientific Reports* **2018** 16165 <https://doi.org/10.1038/s41598-018-34490-9>
22. Tautermann, C.S.; Binder, F.; Buttner, F.H.; Eickmeier, C.; Fiegen, D.; Gross, U.; Grundl, M.A.; Heilker, R.; Hobson, S.; Hoerer, S.; et al. Allosteric Activation of Striatum-Enriched Protein Tyrosine Phosphatase (STEP, PTPN5) by a Fragment-like Molecule. *J. Med. Chem.* **2019**, *62*, 306–316. <https://doi.org/10.1021/acs.jmedchem.8b00857>
23. Pancsa, R.; Zsolyomi, F.; Tompa, P. Co-Evolution of Intrinsically Disordered Proteins with Folded Partners Witnessed by Evolutionary Couplings. *Int. J. Mol. Sci.* **2018**, *19*, 3315 <https://doi.org/10.3390/ijms19113315>
24. Mondal, B.; Reddy, G. Cosolvent Effects on the Growth of Protein Aggregates Formed by a Single Domain Globular Protein and an Intrinsically Disordered Protein. *J. Phys. Chem. B* **2019**, *123*, 1950–1960. <https://doi.org/10.1021/acs.jpcc.8b11128>
25. Supriyo Bhattacharya and Xingcheng Lin Recent Advances in Computational Protocols Addressing Intrinsically Disordered Proteins. *Biomolecules* **2019**, *9*(4), 146; <https://doi.org/10.3390/biom9040146>
26. Yuan, Y.; Pei, J.; Lai, L. Binding site detection and druggability prediction of protein targets for structure-based drug design. *Current pharmaceutical design* **2013**, *19*, 2326-2333, <https://doi.org/10.2174/1381612811319120019>.
27. Jin, F.; Yu, C.; Lai, L.; Liu, Z. Ligand clouds around protein clouds: a scenario of ligand binding with intrinsically disordered proteins. *PLoS computational biology* **2013**, *9*, e1003249. <https://doi.org/10.1371/journal.pcbi.1003249>.
28. Yuan, Y.; Pei, J.; Lai, L. LigBuilder 2: a practical de novo drug design approach. *Journal of chemical information and modeling* **2011**, *51*, 1083-1091, <https://doi.org/10.1021/ci100350u>.
29. Imming, P.; Sinning, C.; Meyer, A. Drugs, their targets and the nature and number of drug targets. *Nature reviews Drug discovery* **2006**, *5*, 821-834, <https://doi.org/10.1038/nrd2132>
30. Tóth, G.; Gardai, S.J.; Zago, W.; Bertonecini, C.W.; Cremades, N.; Roy, S.L.; Tambe, M.A.; Rochet, J.C.; Galvagnion, C.; Skibinski, G.; Finkbeiner, S. Targeting the intrinsically disordered structural ensemble of α -synuclein by small molecules as a potential therapeutic strategy for Parkinson's disease. *PLoS One*, **2014**, *9*, <https://doi.org/10.1371/journal.pone.0087133>
31. Zhu, M., De Simone, A., Schenk, D., Toth, G., Dobson, C. M., & Vendruscolo, M. Identification of small-molecule binding pockets in the soluble monomeric form of the A β 42 peptide. *The Journal of chemical physics*, (2013). 139(3), 07B609_1. <https://doi.org/10.1063/1.4811831>
32. Lobanov, M.Y.; Bogatyreva, N.S.; Galzitskaya, O.V. Radius of gyration as an indicator of protein structure compactness. *Molecular Biology* **2008**, *42*, 623-628, <https://doi.org/10.1134/s0026893308040195>.
33. Ellingson, L.; Zhang, J. Protein surface matching by combining local and global geometric information. *PLoS one* **2012**, *7*, e40540, <https://doi.org/10.1371/journal.pone.0040540>.
34. Liao, K.H.; Chen, K.B.; Lee, W.Y.; Sun, M.F.; Lee, C.C.; Chen, C.Y.C. Ligand-based and structure-based investigation for Alzheimer's disease from traditional chinese medicine. *Evidence-Based Complementary and Alternative Medicine* **2014**, <https://doi.org/10.1155/2014/364819>.
35. Seeliger, D.; De Groot, B.L. Conformational transitions upon ligand binding: holo-structure prediction from apo conformations. *PLoS computational biology* **2010**, *6*, <https://doi.org/10.1016/j.bpj.2009.12.2318>
36. Dhasmana, D.; Singh, A.; Shukla, R.; Tripathi, T.; Garg, N. Targeting Nucleotide Binding Domain of Multidrug Resistance-associated Protein-1 (MRP1) for the Reversal of Multi Drug Resistance in Cancer. *Scientific reports* **2018**, *8*, <https://doi.org/10.1186/s42269-019-0043-8>.
37. Hijazi, I.; Kurgan, L. Improved Prediction of Protein-Small Organic Ligand Binding Sites Via Consensus-Based Ranking with Linear Regression. Proceedings of 3rd International Conference on Environment Energy and Biotechnology, *IPCBE* **2014**, *70*. <https://doi.org/10.7763/IPCBE.2014.V70.7>
38. Darden, T.; York, D.; Pedersen, L. Particle mesh Ewald: An N·log(N) method for Ewald sums in large systems. *The Journal of chemical physics* **1993**, *98*, 10089-10092, <http://dx.doi.org/10.1063/1.464397>.
39. Salomon-Ferrer, R.; Götz, A.W.; Poole, D.; Le Grand, S.; Walker, R.C. Routine microsecond molecular dynamics simulations with AMBER on GPUs. 2. Explicit solvent particle mesh Ewald. *Journal of chemical theory and computation* **2013**, *9*, 3878-3888, <https://doi.org/10.1021/ct400314y>
40. Ryckaert, J.P.; Ciccotti, G.; Berendsen, H.J. Numerical integration of the cartesian equations of motion of a system with constraints: molecular dynamics of n-alkanes. *Journal of computational physics* **1977**, *23*, 327-341, [https://doi.org/10.1016/0021-9991\(77\)90098-5](https://doi.org/10.1016/0021-9991(77)90098-5).
41. Berendsen, H.J.; Postma, J.V.; van Gunsteren, W.F.; DiNola, A.R.H.J.; Haak, J.R. Molecular dynamics with coupling to an external bath. *The Journal of chemical physics* **1984**, *81*, 3684-3690, <https://doi.org/10.1063/1.448118>.

42. Roe, D.R.; Cheatham III, T.E. PTRAJ and CPPTRAJ: software for processing and analysis of molecular dynamics trajectory data. *Journal of chemical theory and computation*. **2013**, 9, 3084-3095, <https://doi.org/10.1021/ct400341p>.

43. Tian, W.; Chen, C.; Lei, X.; Zhao, J.; Liang, J. CASTp 3.0: computed atlas of surface topography of proteins. *Nucleic acids research*, **2018**, 46, W363-W367, <https://doi.org/10.1016/j.bpj.2017.11.325>

44. Kabsch, W.; Sander, C. Dictionary of protein secondary structure: pattern recognition of hydrogen-bonded and geometrical features. *Biopolymers* **1983**, 22, 2577-2637, <https://doi.org/10.1002/bip.360221211>.

Krieger, E.; Vriend, G.; Spronk, C. YASARA–Yet Another Scientific Artificial Reality Application. YASARA. org **2013**, 993.

6. ACKNOWLEDGEMENTS

This work was supported by the Science and Engineering Research Board (SERB), Government of India (EMR/2017/005383). DD and MK thanks DST-SERB for the fellowship.



© 2020 by the authors. This article is an open access article distributed under the terms and conditions of the Creative Commons Attribution (CC BY) license (<http://creativecommons.org/licenses/by/4.0/>).

Supplementary files

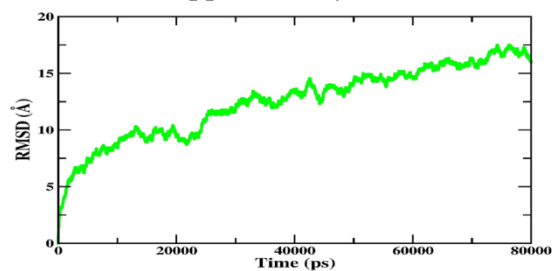
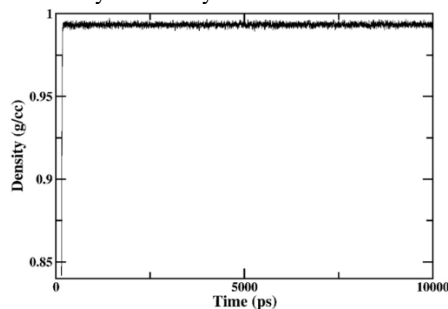
Figure S1. RMSD analysis for α -synuclein as a function of simulation time

Figure S2. Density of the system as a function of simulation time period.

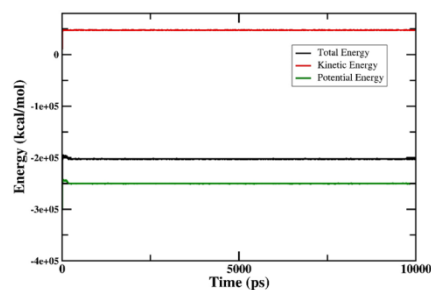


Figure S3. Energy (Total energy, Potential energy and Kinetic energy) of the system as a function of simulation time period.

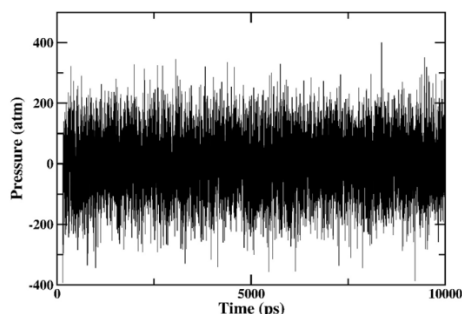


Figure S4. Pressure of the system as a function of simulation time period.

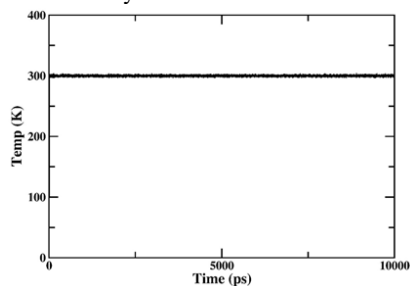


Figure S5. Temperature of the system as a function of simulation time period

Table S1. Binding Pocket Information for the conformers of α -synuclein.

BINDING POCKET INFORMATION: L1				
POCKET ID	AREA (Å)	VOLUME (Å)	NUMBER OF RESIDUES	NUMBER OF ATOMS
1	193.56	984.96	12	46
2	158.94	484.77	12	41
3	19.93	60.39	4	7
4	21.62	14.97	4	13
5	12.98	11.36	5	14

Screening of druggable conformers of α -synuclein using molecular dynamics simulation

6	17.84	10.64	4	13
7	16.53	8.49	4	13
8	10.52	7.73	5	8
9	19.52	7.36	6	13
10	26.98	5.26	8	20
11	7.57	0.93	6	11
12	1.42	0.25	3	5
13	1.38	0.16	4	4
14	1.51	0.14	4	7
15	0.38	0.00	4	6

BINDING POCKET INFORMATION: L2

POCKET ID	AREA (SA)	VOLUME (SA)	NUMBER OF RESIDUES	NUMBER OF ATOMS
1	178.50	749.40	16	50
2	33.16	17.73	5	13
3	27.29	14.46	5	14
4	16.42	14.45	4	11
5	13.94	8.26	4	11
6	5.37	6.53	5	7
7	27.47	4.56	8	21
8	10.64	4.55	4	6
9	2.71	0.42	5	7
10	3.76	0.40	3	6
11	4.00	0.24	6	11
12	0.62	0.06	3	4
13	0.78	0.02	4	8
14	0.36	0.00	5	6
15	0.01	0.00	4	5
16	0.01	0.00	3	4
17	0.00	0.00	3	4

BINDING POCKET INFORMATION: L3

POCKET ID	AREA (SA)	VOLUME (SA)	NUMBER OF RESIDUES	NUMBER OF ATOMS
1	137.68	733.85	10	30
2	50.50	18.02	10	33
3	16.15	11.97	4	10
4	19.01	11.88	4	12
5	26.05	9.91	5	12
6	16.39	8.25	5	13
7	9.65	6.58	4	7
8	5.74	0.75	6	12
9	5.83	0.52	6	10
10	0.95	0.11	3	4
11	0.06	0.00	4	5

BINDING POCKET INFORMATION: L4

POCKET ID	AREA (SA)	VOLUME (SA)	NUMBER OF RESIDUES	NUMBER OF ATOMS
1	143.66	770.42	14	32
2	12.25	286.00	5	5
3	12.62	8.27	4	10
4	27.92	7.15	7	15
5	12.39	6.77	5	8
6	2.70	6.51	4	9
7	5.85	5.12	4	6
8	9.47	4.18	4	7
9	20.99	3.85	8	20
10	9.38	2.41	4	8
11	3.64	2.00	3	5
12	0.85	0.15	3	4
13	1.43	0.11	4	6
14	0.97	0.08	4	5
15	0.19	0.00	3	5
16	0.14	0.00	3	4
17	0.09	0.00	4	5
18	0.06	0.00	3	4
19	0.00	0.00	4	4

BINDING POCKET INFORMATION: L5

POCKET ID	AREA (SA)	VOLUME (SA)	NUMBER OF RESIDUES	NUMBER OF ATOMS
1	178.30	1063.89	14	41
2	33.12	21.01	6	13
3	23.05	15.25	4	15
4	33.81	13.09	7	20
5	8.47	9.83	4	7
6	23.73	2.49	8	21
7	3.74	0.68	3	6
8	4.25	0.50	5	10
9	0.71	0.17	2	4
10	1.51	0.16	4	4

11	0.45	0.03	4	4
12	0.21	0.01	3	4
13	0.21	0.00	3	5
14	0.20	0.00	3	4
15	0.05	0.00	3	4
16	0.03	0.00	4	4

BINDING POCKET INFORMATION: M1

POCKET ID	AREA (SA)	VOLUME (SA)	NUMBER OF RESIDUES	NUMBER OF ATOMS
1	252.50	864.36	18	46
2	25.87	20.37	6	18
3	12.76	14.29	7	13
4	25.48	9.64	7	14
5	6.69	2.46	4	9
6	8.18	2.35	4	10
7	6.66	0.60	6	14
8	0.15	0.03	3	4
9	13.24	-0.77	4	10

BINDING POCKET INFORMATION: M2

POCKET ID	AREA (SA)	VOLUME (SA)	NUMBER OF RESIDUES	NUMBER OF ATOMS
1	50.09	88.77	7	16
2	6.23	2.62	4	6
3	6.86	1.56	7	10
4	5.47	1.29	5	7
5	2.72	0.43	4	6
6	1.23	0.25	4	7
7	2.78	0.13	4	6
8	1.92	0.12	3	5
9	0.40	0.00	3	4
10	0.13	0.00	3	6

BINDING POCKET INFORMATION: M3

POCKET ID	AREA (SA)	VOLUME (SA)	NUMBER OF RESIDUES	NUMBER OF ATOMS
1	473.13	2505.87	26	88
2	16.50	79.05	4	7
3	48.09	78.88	7	14
4	-0.29	0.12	3	6
5	0.81	0.11	3	4
6	0.62	0.03	5	5
7	0.37	0.01	4	6
8	0.39	0.00	4	5
9	0.12	0.00	3	5
10	0.01	0.00	3	4
11	0.01	0.00	3	4

BINDING POCKET INFORMATION: M4

POCKET ID	AREA (SA)	VOLUME (SA)	NUMBER OF RESIDUES	NUMBER OF ATOMS
1	15.61	77.29	4	5
2	29.58	12.04	6	17
3	27.65	7.96	6	14
4	4.24	3.45	3	6
5	6.73	1.04	4	6
6	-0.88	0.84	4	7
7	2.45	0.35	4	4

BINDING POCKET INFORMATION: M5

POCKET ID	AREA (SA)	VOLUME (SA)	NUMBER OF RESIDUES	NUMBER OF ATOMS
1	307.12	2134.89	22	64
2	152.19	506.34	11	33
3	44.26	104.99	7	14
4	16.62	5.30	7	16
5	17.33	2.23	7	16
6	1.63	0.37	3	5
7	1.42	0.24	4	5
8	0.45	0.21	2	4
9	1.22	0.17	3	5
10	2.06	0.15	4	7
11	1.30	0.10	4	7
12	1.43	0.04	4	7
13	0.30	0.01	4	5
14	0.51	0.00	3	5
15	0.11	0.00	4	4

BINDING POCKET INFORMATION: H1

POCKET ID	AREA (SA)	VOLUME (SA)	NUMBER OF RESIDUES	NUMBER OF ATOMS
1	12.49	124.01	4	6
2	25.51	122.40	4	9
3	57.36	70.22	8	22

Screening of druggable conformers of α -synuclein using molecular dynamics simulation

4	21.98	46.99	5	10
5	16.38	14.53	4	8
6	2.53	3.78	3	5
7	9.26	1.16	4	10
8	1.89	0.10	4	6
9	0.74	0.04	2	4
10	0.59	0.04	2	4
11	0.62	0.03	4	6

BINDING POCKET INFORMATION: H2

POCKET ID	AREA (SA)	VOLUME (SA)	NUMBER OF RESIDUES	NUMBER OF ATOMS
1	27.44	135.05	4	9
2	50.20	58.95	8	21
3	49.60	39.36	8	17
4	1.90	28.35	3	4
5	1.04	0.22	2	4
6	0.41	0.05	2	4
7	0.79	0.04	5	5

BINDING POCKET INFORMATION: H3

POCKET ID	AREA (SA)	VOLUME (SA)	NUMBER OF RESIDUES	NUMBER OF ATOMS
1	15.33	157.75	5	7
2	39.06	128.30	5	12
3	13.80	61.39	4	9
4	71.76	60.45	9	23
5	15.94	29.62	4	5
6	21.85	19.34	6	13
7	3.87	1.18	3	6
8	2.45	0.35	4	11
9	0.92	0.04	3	8
10	0.29	0.01	5	6
11	2.64	-0.38	4	6

BINDING POCKET INFORMATION: H4

POCKET ID	AREA (SA)	VOLUME (SA)	NUMBER OF RESIDUES	NUMBER OF ATOMS
1	52.79	191.90	5	15
2	26.01	75.72	6	12
3	45.78	47.28	6	15
4	43.92	42.65	7	15
5	50.52	41.42	8	18
6	5.77	1.87	4	7
7	4.45	0.51	6	10
8	4.42	0.07	4	9
9	0.24	0.00	3	5

BINDING POCKET INFORMATION: H5

POCKET ID	AREA (SA)	VOLUME (SA)	NUMBER OF RESIDUES	NUMBER OF ATOMS
1	17.70	96.24	4	6
2	56.92	56.07	7	20
3	60.50	48.41	8	21
4	3.47	0.84	3	9
5	1.83	0.30	3	7
6	1.35	0.20	3	5
7	1.23	0.08	3	8
8	0.92	0.03	4	5